



HAL
open science

The InSight Blind Test: An Opportunity to Bring a Research Dataset into Teaching Programs

Julien Balestra, Jean-Luc Berenguer, Florence Bigot-cormier, Françoise Courboux, Lucie Rolland, David Ambrois, Martin van Driel, Philippe Lognonne

► **To cite this version:**

Julien Balestra, Jean-Luc Berenguer, Florence Bigot-cormier, Françoise Courboux, Lucie Rolland, et al.. The InSight Blind Test: An Opportunity to Bring a Research Dataset into Teaching Programs. Seismological Research Letters, 2020, 91 (2A), pp.1064-1073. 10.1785/0220190137 . hal-02461538

HAL Id: hal-02461538

<https://hal.science/hal-02461538v1>

Submitted on 24 Nov 2020

HAL is a multi-disciplinary open access archive for the deposit and dissemination of scientific research documents, whether they are published or not. The documents may come from teaching and research institutions in France or abroad, or from public or private research centers.

L'archive ouverte pluridisciplinaire **HAL**, est destinée au dépôt et à la diffusion de documents scientifiques de niveau recherche, publiés ou non, émanant des établissements d'enseignement et de recherche français ou étrangers, des laboratoires publics ou privés.

1 **The InSight Blind Test: an Opportunity to Bring a Research Dataset into Teaching**
2 **Programs**

3

4 Julien Balestra⁽¹⁾, Jean-Luc Berenguer^(2,3), Florence Bigot-Cormier⁽⁴⁾, Françoise Courboulex⁽²⁾,
5 Lucie Rolland⁽²⁾, David Ambrois⁽²⁾, Martin Van Driel⁽⁵⁾ and Philippe Lognonné⁽⁶⁾

6

7 1) Université Côte d'Azur, Campus Valrose, Bâtiment L, 28 Avenue de Valrose, 06108 Nice
8 CEDEX 2, France

9 2) Université Côte d'Azur, CNRS, Observatoire de la Côte d'Azur, IRD, Géoazur, UMR7329,
10 250 rue Albert Einstein, Sophia Antipolis 06560 Valbonne, France

11 3) Centre International De Valbonne, BP 97, 06902 Sophia Antipolis, Cedex, France

12 4) French School of Shanghai, 350 Gao Guang Road, Qingpu District, Shanghai 201702, China

13 5) Institute of Geophysics, ETH Zürich, Sonneggstrasse 5, 8092, Zurich, Switzerland

14 6) Université de Paris, Institut de physique du globe de Paris, CNRS, F-75005 Paris, France

15

16 Corresponding author: julien.balestra@univ-cotedazur.fr

17

18

19

20

21

22 Abstract

23 On November 26, 2019, SEIS, the first broadband seismometer designed for the Martian
24 environment (Lognonné et al., 2019) landed on Mars thanks to NASA’s InSight mission. On
25 April 6, 2019 (sol 128), the InSight Science team detected the first historical “marsquake”
26 (NASA news release). Before it was recorded, the InSight Science team developed the InSight
27 Blind Test (hereafter IBT), **which consists of a 12-month period of continuous waveform data**
28 **combining realistic estimates of martian background seismic noise, 204 tectonic and 35 impact**
29 **events (Clinton et al., 2017).** This project was originally designed to prepare scientists for the
30 arrival of real data from the upcoming InSight mission. This paper presents the work carried
31 out by middle and high school students during this challenge. This project offered schools the
32 opportunity to participate in and strengthen the link between secondary schools and universities.
33 The IBT organizers accepted the approach to enable fourteen schools to take part in this
34 scientific challenge. After a training process, each school analyzed the IBT dataset to contribute
35 to the collaborative School Team catalog. The schools relied on a manual procedure combining
36 analyses in time and frequency domains. At the end, a combined catalog was submitted as one
37 of the IBT entries. The IBT organizers then assessed the catalog submitted by the consortium
38 of schools together with the results from science teams (Van Driel et al., 2019). The schools
39 achieved a total of 15 correct detections over a short period. **While this number may seem**
40 **modest compared with the 239 synthetic marsquakes included in the IBT waveform data, these**
41 **correct detections were entirely made during class time.** All in all, the students seemed to be
42 fully engaged, and this exercise seemed to increase their scientific inquiry skills in order to
43 fulfill their task as a team.

44

45

46 **Introduction**

47 The InSight mission includes an education and outreach program (E&O) in each partner
48 country. In France, the E&O is carried out by the Géoazur education team. Many pedagogical
49 resources were proposed for this mission, including aspects from launch to landing. The IBT
50 was an excellent opportunity to prepare students to work on future Martian seismograms. The
51 organizers prepared a synthetic dataset of continuous waveforms and invited participants to
52 detect both tectonic and impact seismicity, along with different sources of noise (Murdoch et
53 al., 2017a, 2017b, Kenda et al., 2017). **Note that:**

- 54 - the IBT stopped on February 2018,
- 55 - the continuous synthetic signal was considered for a fictional year 2019 (from January
56 1 to December 31).

57 **All mentions of data from 2019 concern this fictional year.**

58 The objective was to prepare research teams interested in developing detection procedures and
59 assess the quality of their work by comparing the seismicity catalog they produced with the IBT
60 synthetic seismicity catalog.

61 Given that using data in schools from scientific research has shown a positive impact on
62 students (Zollo et al., 2014, Bigot-Cormier and Berenguer, 2017), we asked the IBT organizers
63 if the participation of schools was possible. We proposed having the students determine key
64 event parameters such as date, arrival time of seismic waves, epicentral distance and back-
65 azimuth direction, terms used in the French educational curriculum. The organizers accepted
66 this format. The School Team was composed of 14 schools either in France or abroad (Fig. 1),
67 all of which are part of the French educational seismic network (Courboulex et al., 2012). Catts
68 Pressoir Middle School is a Haitian school, but their teaching program is similar to that of the
69 French curriculum followed by the other schools. The IBT was considered to be an excellent

70 scientific dataset for teaching lessons and was aligned with a series of expected skills, which
71 will be highlighted throughout this study.

72 One of the expected skills is to identify, extract and organize information from scientific data.
73 In middle school lessons, earthquakes are taught as being the result of the Earth's internal
74 activity. Students learn that ground motions during an earthquake are due to different waves
75 shaking the surface. A typical class exercise is to identify different seismic phases in a
76 seismogram. During subsequent high school lessons, a classic exercise is to determine the
77 arrival times of seismic P and S waves in order to locate the epicenter. We were strongly
78 convinced that the data from the IBT could be used instead of these classic exercises as a
79 previously unseen dataset. Furthermore, it was felt that student motivation would be increased
80 by knowing that the InSight science team would analyze their results.

81 At the start of this project, a training process was required to efficiently prepare students for the
82 upcoming synthetic data analysis.

83

84 **Student Training Process**

85 *Real Earth and Synthetic Mars Data*

86 In order to train students and increase their skills in seismic signal analysis, we provided
87 students with two newsletters in October 2017. Each document was in PDF format, with
88 numerical data attached. In this study, all numerical datasets were analyzed with
89 SeisGram2K80_ECOLE.jar (SG2K80, Lomax A., 2000) software. A specific velocity model
90 was implemented by A. Lomax (from Sohn and Spohn, 1997).

91 The task approach was to study examples of signal processing. Students first worked on
92 decimation and its effect on seismic data. We provided real seismograms recorded at the BLOR

93 education station (“Lycée de la Montagne” high school in Valdeblore, France). The earthquakes
94 considered were:

- 95 - the April 7, 2014, Barcelonnette earthquake (Mw 4.9, France, 0.6° epicentral
96 distance);
- 97 - the April 16, 2016, earthquake (Mw 7.8, Ecuador region, 87.6° epicentral distance).

98 Students then worked on bandpass filtering and frequency content. We provided synthetic
99 signals from the IBT. The proposed **fictional time periods** were:

- 100 - January 10 to 15, 2019;
- 101 - July 15, 2019;
- 102 - September 22, 2019.

103 We rotated these signals into the north, east, and Z (vertical) directions from metadata provided
104 by the IBT organizers using the ObsPy packages (Krischer et al., 2015). No instrumental
105 correction for response was applied.

106

107 *Decimation of Seismic Signals: an Exercise to Manipulate, Experiment, and Understand the*
108 *Nature of the Data Used*

109 The first exercise was designed to help students become familiar with the nature of the IBT
110 dataset, **especially with the difficulty of working with decimated seismic data**. The SEIS
111 seismometer stores data at 100 Hz. At the time of the IBT, the initial sampling rate retained for
112 future real data transmission was 2 Hz. **This corresponds to a volume of data transfer**
113 **guaranteed by the NASA**. The educational seismic stations used by students typically store
114 ground motion at 50 Hz. Therefore, the first exercise was to introduce the synthetic data
115 corresponding to decimated data, i.e. with lower resolution than the raw data. **Students** worked

116 on the Barcelonnette earthquake decimated to 2 Hz. Decimation was carried out using the
117 Python ObsPy software package (with an anti-aliasing low-pass filter). Figure 2a shows raw
118 and decimated seismograms (vertical component). Change in amplitude was the first effect
119 observed by students. They understood that samples were missing, which implies that
120 information about ground motion was missing. Zooming in with SG2K80 also allowed them to
121 observe changes in shape (Fig. 2b). After these first manipulations, students worked on the
122 teleseismic event. At first they observed no significant changes in amplitude between the raw
123 and the decimated signal (Fig. 2c). They observed that the decimation had very little effect on
124 the signal. Zooming in enabled them to observe small differences due to the anti-aliasing
125 prefiltering (Fig. 2d).

126 **This first analysis of changes of seismogram shapes enabled students to understand the effect**
127 **of this kind of processing on raw data. Understanding the link between the content of a dataset,**
128 **and the information that can be extracted from it, is an important skill required in French**
129 **educational programs.** Moreover, students were also able to imagine how difficult it would be
130 to analyze future real Martian seismograms decimated to 2 Hz.

131 This first step concluded with the introduction of the relationship between the shape and period
132 of the signal. Signals were described as being composed of tighter or looser arcs, with tight arcs
133 corresponding to short periods and broad arcs corresponding to long periods, following the
134 approach of Bigot-Cormier and Berenguer (2017). This allowed us to introduce a second step
135 based on frequency analysis.

136

137 *Bandpass Filter and Spectrogram: Use of Digital Tools to Identify Seismic Waves*

138 The frequency content of seismograms was introduced in response to the question raised by
139 students: “How will scientists be able to detect seismic activity?”. For both middle and high

140 school students, the use of a bandpass filter is unusual. Understanding the calculation of
141 spectrograms is too difficult, and it is not a subject in the French curriculum. However, students
142 are expected to use digital processing software. SG2K80 proposes tools to filter seismograms
143 and to compute a corresponding spectrogram, which was introduced as a data processing
144 method to highlight the frequency content of the continuous signals. To become familiar with
145 these different aspects, students were invited to work with the synthetic seismogram on January
146 12, 2019 (IBT fictional day, vertical component, Fig. 3). Note that any mentions below of a
147 synthetic seismogram refer to the IBT, except seismograms computed in the study of Bozdağ
148 et al. (2017).

149 Students started this new activity by applying bandpass filters to understand their effects on the
150 seismograms analyzed. Two frequency intervals were provided:

- 151 - from 0.001 Hz to 0.01 Hz (lf-bp for low frequencies bandpass),
- 152 - from 0.01 Hz to 1.0 Hz (hf-bp for high frequencies bandpass).

153 The frequency of 1 Hz corresponds to the Nyquist frequency, i.e. the maximum frequency that
154 can be analyzed for a decimation to 2 Hz. The comparison of these three signals (raw and
155 filtered) allowed students to highlight different points of the filtering process. By applying lf-
156 bp filtering, they observed that the very long period arc observed in Figure 3a was filtered out.
157 They also observed a long duration event (Fig. 3b). With hf-bp filtering this long duration event
158 was always observed along with a later and shorter duration event (Fig. 3c).

159 This kind of processing is consistent with the skills required by the educational curriculum.
160 Students showed they understood that:

- 161 - events (seismic, atmospheric, etc.) observed in a seismogram have their own frequency
162 characteristics;

- 163 - the filtering process is used to try to highlight expected or searched events in
- 164 seismograms;
- 165 - the shape of seismograms varies according to removed frequencies.

166 Although, in this case, a filtering process allows the detection of significant events, we invited
167 students to analyze the computed spectrogram from the raw seismogram (SG2K80 spectrogram
168 tool, Fig. 3d and 3e). Students observed that the long and later short events are easier to detect
169 by displaying the frequency content of the seismogram reading. Figure 3d shows that the two
170 events are highlighted by an increased amplitude for specific frequencies (about 0.1 Hz for the
171 long event, up to 0.8 Hz for the shorter event), which indicates a significant change in ambient
172 ground motion.

173 Students understood that hidden synthetic marsquakes could be easier to detect by processing
174 data. To go even deeper into the analysis, zooming in on the late and short event was proposed
175 (Fig. 3e). Students observed that the long duration signal is composed of a frequency content
176 different from the shorter duration event. They also observed an extended coma-like shape (Fig.
177 3e, black dashed ellipse). From discussions with seismologists at Géoazur (who also
178 participated in the IBT as one of the challengers, Van Driel et al., 2019), this specific shape was
179 designated as the signature of Rayleigh waves. These surface waves have a velocity that is
180 dependent on their frequencies. Thus, some Rayleigh waves arrive earlier and some arrive later,
181 which reflects their dispersion. This specific shape was used to determine and identify them.

182 The frequency content of body waves was also approached. From the July 15 (M4.3) and the
183 September 22 (M5.0) synthetic events, the frequency content of body waves was considered as
184 ranging from 0.3 Hz to 0.9 Hz (higher than the frequency content of Rayleigh waves). The work
185 on seismic phases with these large synthetic events was considered as sufficient to help students
186 to detect smaller nearby quakes with higher frequency content.

187 The training process stopped here for middle school students. According to their educational
188 curriculum, they were ready to analyze synthetic data. Their goal was to identify arrival times
189 of seismic waves and to propose their part of the School Team catalog of seismicity. It was
190 possible to extend this analysis for high school students, thus the second newsletter was given
191 to them.

192

193 *Guided Analysis and Interpretation of Synthetic Signals from the InSight Blind Test: Skills*
194 *Expected for High School Students*

195 *A. Estimation of the epicentral distance based on Rayleigh wave arrival times*

196 **Extracting information from scientific datasets is an expected skill for high school students.**

197 Locating the epicenter is a good exercise for this, and even more so if the dataset comes from a
198 current scientific project. Typically, seismic events are located by analyzing P and S wave
199 arrival times from three or more seismic stations. One aim of the second newsletter given to
200 students was to introduce a location technique using only one three-component station, without
201 any knowledge of an accurate deep structure of the planet, and without the origin time. We
202 proposed using successive Rayleigh wave arrival times (Panning et al., 2015). Hereafter this
203 paper will use the following notations (Fig. 4a and 4b):

- 204 - t_1 : the first arrival time of Rayleigh waves at the virtual station, i.e. the shortest surface
205 travel time between the epicenter and the station (LR1, for Long-period Rayleigh 1);
- 206 - t_2 : the second arrival time of Rayleigh waves at the station, i.e. the longest surface travel
207 time between the epicenter and the station (LR2);

208 - t3: the third arrival time of Rayleigh waves at the station, i.e. the shortest surface travel
209 time between the epicenter and the station, plus a complete surface trip around the planet
210 (LR3).

211 The method from Roques et al. (2016) was used to illustrate this approach (Fig. S1). The
212 synthetic seismograms used in this method came from the study by Bozdağ et al. (2017). They
213 were computed at virtual stations along the Mars equator, spaced by 20°. The mathematical
214 formula to compute epicentral distance from t1, t2, and t3 arrival times is:

$$215 \quad \text{Epicentral distance} = \frac{t3-t2}{t3-t1} * \pi * R_{planet} \quad (1)$$

216 where R_{planet} is the radius of the considered planet. Distances are in kilometers and arrival
217 times are in seconds. This work was interesting because distances and origin times were known.
218 Students were easily able to confirm their results.

219 We then invited students to work with an unknown event from the IBT using the synthetic
220 seismogram from September 22, 2019 (Fig. 4b). We chose this event because the analysis of its
221 frequency content showed specific signatures considered as a marker of Rayleigh waves.
222 Students were able to observe the different wave trains in the time domain, which presented
223 specific signatures in the frequency domain. From this analysis and by picking the three
224 passages of Rayleigh waves, students estimated an epicenter located at 35.5° from the station.
225 Thus they understood that this approach is not enough to locate the event. They estimated a
226 distance, but the direction was missing. This aspect was the subject of the last training exercise.

227

228 *B. Azimuth and back-azimuth estimation from the rotation of horizontal components*

229 This last exercise was introduced using a simple hands-on activity. We provided electronic
230 accelerometers and the RISSC© (Record Interface Sensors at School, see Data and Resources)

231 interface. This educational interface displays records from each component in real time, which
232 are identified with a sticky label (Fig. S2). The accelerometers were fixed on a table, and
233 students followed two procedures: first, to apply an impact parallel to the table plane in the X
234 direction of the device, and second, to apply an impact in the Y direction of the device. Using
235 records displayed with RISSC, students observed the difference in amplitude of each
236 component and concluded that the maximum amplitude is observed in the main direction of
237 wave propagation. In class, students then reviewed the relationship between azimuth and back-
238 azimuth. **SG2K80 software includes a tool to compute the angle value of the azimuth from the**
239 **first P wave amplitude on horizontal components (Fig. 5).** This function allows recomputed
240 signals to be displayed after a chosen rotation value (as a virtual rotation of the sensor in the
241 geographical coordinate system). Figure 5a shows the first P wave on each component, without
242 rotation. Figure 5b shows a flat P wave on the East component for a 65° (clockwise) rotation.
243 This is also the value for which the P wave amplitude is maximal on the North component.
244 Students understood that this virtual rotation of the sensor allows them to determine the
245 direction for which the first ground motion is maximal on one of the horizontal components
246 and zero on the other.

247 The last training exercise involved determining the back-azimuth. From the P wave polarity
248 (upwards) on the vertical component, students calculated a back-azimuth equal to 245°. The
249 final catalog of the IBT was not available at the moment of this training process. Students waited
250 for the publication of the solution to evaluate their first detection. Figure S3 shows the results
251 of this training exercise validated after the publication of the true catalog. They used the
252 EduCarte-Mars geographical information system (GIS) to display the results of location. The
253 specific Mars digital field model was implemented by A. Lomax.

254 This last activity completed the schools' training for the IBT. The fourteen schools then each
255 received one month of non-overlapping synthetic data and started their analyses during their
256 teaching sessions.

257

258 **Blind Test Independent Data Analysis and the Creation of the School Team Catalog**

259 The analysis phase started at the beginning of November, 2017, and ended in January, 2018.

260 This period was long enough for teachers to integrate this challenge (training and analysis
261 phases) into their official teaching hours. Students worked for six to ten hours on this project.

262 We now describe two activities performed by students at each school.

263

264 *A Daily Atmospheric Signature*

265 During the one-year-long synthetic seismogram, disturbances in the continuous signal were not
266 exclusively due to traveling seismic waves. For example, environmental noise (Spiga et al.
267 2010) was added in order to create a signal that was as realistic as possible (Clinton et al., 2017),
268 with the associated modeled seismic noise originating from the interaction of the environment
269 with the lander or the ground (Murdoch et al, 2017a, 2017b, Kenda et al., 2017). See Spiga et
270 al. (2018) for a general review of atmospheric seismic noise and Lognonné et al. (2019) for
271 noise shielding on the SEIS instrument.

272 During the training steps, students identified an unknown long event in the synthetic
273 seismogram that occurred on January 12, 2019 (fictional day from the IBT). During the analysis
274 phase, students observed that in fact this long event occurred each day, but not at the same hour.
275 Students asked us for an explanation of this phenomenon, and we submitted the question to a
276 researcher, who gave them the following explanation. The sun warms the surface of Mars,

277 which causes thermal agitation (convection) near the surface. At nightfall, the surface cools
278 because the sun no longer warms it and convection stops. The wind blows, but there are no
279 rapid turbulent fluctuations that produce this atmospheric noise. The observed time lag can be
280 explained by the length of Martian days, which last approximately 24 hours and 39 minutes.

281 One of our aims was reached through this interaction, i.e. to create a link between students and
282 researchers, and to improve the students' scientific inquiry skills.

283

284 *Estimation of the Epicentral Distance of an Unknown Event That Occurred on July 15, 2019*

285 This section presents the analysis provided by high school students of the event of July 15, 2019
286 (fictional day from the IBT). They were able to observe different wave trains on the vertical
287 component and they clearly identified two Rayleigh wave signatures in the frequency domain
288 (Fig.7). However, without a clear third signature from the whole day's seismogram, they
289 decided to pick a third Rayleigh wave at the start of an increase of the scale amplitude around
290 7:00 a.m. By picking these three Rayleigh waves, they obtained an epicentral distance equal to
291 90.5° (from the corresponding SG2K80 tool). The correct epicentral distance was 90.94° . The
292 slight change in amplitude in the frequency domain is probably due to the start of daily
293 atmospheric disturbances, but the lower value of the bandpass filter value applied by students
294 (0.1 Hz to 1 Hz, Fig. 7) was too high to highlight this daily event. However, we appreciated
295 their approach and their thinking through the use of the analysis processes they learned during
296 the training phase.

297

298

299

300 **Discussion**

301 The teachers' geophysical skills enabled the project to be properly completed. They have
302 attended various workshops on the subject during their careers and have already worked on
303 educational projects based on seismic data. The teachers included this challenge in their
304 teaching time and at their convenience. As mentioned above, the students worked at most about
305 ten hours. The schools worked independently during the analysis phase. The main reason for
306 this was that teachers chose the allocated period to work on synthetic data. At the end of January
307 2018, the catalog from the School Team was provided to the IBT organizers. This catalog
308 (Table 1) was then compiled in Van Driel et al. (2019) (Fig. S4). The School Team catalog
309 contained fifteen correct events: thirteen quakes and two impacts. Six high schools and two
310 middle schools found these events. The other schools gave wrong detections. For the students,
311 the main constraints were the available tools and the limited time to work on this challenge.

312 Detected events were located between 700 km and 8400 km from the chosen seismometer
313 location. The detected synthetic events had magnitudes ranging from 2.5 to 5. The closest event
314 in the true catalog (191 km, M2.5) was not detected. Two events of magnitude 2.5 and 2.6 were
315 detected. Their epicentral locations were 724 km and 713 km respectively. Seven events,
316 ranging from magnitude 3 to magnitude 4, were detected. Their epicentral locations ranged
317 from 1000 km to 6500 km. One event with a magnitude higher than 4 was detected (at 5379
318 km). The larger event (M5.0, 2000 km) occurred on September 22 (studied during the training
319 process) was also added to the catalog. Two impacts were also detected, the stronger impact on
320 October 24, and a weaker impact on October 25.

321 In total, 103 events were compiled in the School Team catalog. Changes in the amplitude and
322 frequency of the continuous signal often were considered as seismic waves, because the
323 corresponding computing spectrogram showed changes in amplitudes. These false detections
324 could be a result of the very short teaching time allowed in the training and analysis phases.

325 These many false detections could be the starting point for a new educational project with a
326 dataset from the IBT. Future student groups could start analyzing why these false detections
327 were made. The aim would be to improve the training phase documentation in order to facilitate
328 the dismissal of some events in the continuous signal.

329 This study could be conducted once again at middle schools and high schools, which could be
330 paired. Middle school students would work on identifying seismic waves, and the high school
331 students would have two objectives: i) validate or invalidate detections, ii) try to estimate a
332 location for detections considered as true. This networking would allow for an increase of
333 educational skills. Furthermore, annual educational projects are planned in new educational
334 programs for high schools. A longer period to work on this challenge would be useful to enable
335 us to compare the quality of the catalog provided.

336

337 **Conclusion**

338 Of course, our ambition was not to compete with other science teams. Our main goal was to
339 highlight the IBT dataset to school students. **This objective was achieved because of motivated**
340 **teachers who decided to engage their students in this challenge.** No written evaluation was
341 specifically carried out, but all teachers reported their satisfaction with the work provided by
342 students. They were also satisfied that they had been able to include this dataset in their own
343 activities. Figures S5a and S5b show pictures of students working on this challenge. Even the
344 few students with learning difficulties responded well to the project, showing a good level of
345 involvement and were engaged in class discussions. We think that the reason was that the
346 framework was out of the ordinary. The aim was not to work on a typical exercise, but to suggest
347 a catalog to the InSight Science Team.

348 Teacher feedback focused on the great impact of the IBT on classroom dynamics. It allowed
349 students to develop the following main skills:

- 350 - practice a scientific approach;
- 351 - demonstrate observation skills, curiosity, critical thinking;
- 352 - experience autonomy;
- 353 - communicate in scientifically appropriate language: oral, written, graphic, numerical.

354 Middle school students showed that they were able to detect synthetic events, even though their
355 scientific background was less developed than that of high school students. This point highlights
356 that involvement and seriousness, and not the age of students, were the main determining
357 aspects to properly carry out this challenge.

358 The French EduMed Observatory educational project organized a seminar in the French
359 Géoazur laboratory. Students from high schools came to present the classwork they had carried
360 out during their school year. One group presented their work from the September 22 synthetic
361 quake (Fig. S5c). They presented their picks of Rayleigh waves and their estimate of the
362 epicentral location. They also presented their work on 1D velocity models proposed for the IBT
363 (Clinton et al., 2017). They estimated the origin time from t_1 , t_2 , and t_3 , and then they calculated
364 the velocity of the first P wave. They also considered the following starting models: i) a
365 homogeneous planet, ii) the source located at the surface, iii) a seismic ray as a straight line
366 between the source and the station. They also computed a theoretical depth reached by this first
367 “straight” P wave. By comparing their results with velocity models published in Clinton et al.
368 (2017), they understood that they had chosen a wrong starting velocity model, and learned about
369 how seismic datasets are used to understand the deep structure of Mars. Although they did not
370 succeed in determining the model that was used for the IBT, they showed that they developed
371 many expected skills by working on this dataset.

372 Student teams are now ready and looking forward to analyzing real data from Mars. In addition,
373 educators should keep in mind that even more challenging seismic signals are expected to be
374 recorded on Mars, with a majority of small, nearby marsquakes (higher frequency content,
375 lower signal noise ratio). A couple of teleseismic events will hopefully reveal the deep interior
376 of the planet.

377

378 **Data and Resources**

379 Seismograms from the two earthquakes recorded at the BLOR educational seismic station,
380 SeisGram2K80_ECOLE.jar software, and the RISSC interface are available on the EduMed
381 Observatory website:

382 - the Barcelonnette earthquake:

383 http://edumed.unice.fr/fr/data-center/seismo/donnees-seismo/2014-04-07-5_0_barcelonnette

384 - The Ecuador earthquake:

385 http://edumed.unice.fr/fr/data-center/seismo/donnees-seismo/2016-04-16-7_8_ecuador

386 - SG2K80:

387 <http://edumed.unice.fr/fr/contents/news/tools-lab/SeisGram2K>

388 - Record Interface Sensors at School (developed by David Ambrois):

389 <http://edumed.unice.fr/fr/contents/news/tools-lab/RISSC>

390

391 EduMed Observatory is funded by the University of Côte d'Azur – JEDI Investments in the
392 Future project managed under reference number ANR-15-IDEX-01.

393 Synthetic seismograms for the IBT are available from the specific ETH website
394 (<http://blindtest.mars.ethz.ch>).

395 The synthetic data presented in this study and EduCarte software (Mars version) are also
396 available on the French InSight educational website supported by the Centre National d'Etudes
397 Spatiales (CNES):

398 - InSight Blind Test dataset:

399 https://insight.oca.eu/images/InSight_Medias/zip/blindtest_daily_synthetic_data.zip

400 - Synthetic data from Bozdağ et al. (2017):

401 https://insight.oca.eu/images/InSight_Medias/zip/data/data-bozdag-2017.zip

402 - EduCarte Mars (© A. Lomax and J.L. Berenguer):

403 https://insight.oca.eu/images/InSight_Medias/zip/software/Educarte-Mars-3.3.0X18.zip

404

405 **Acknowledgments**

406 We are especially grateful to the IBT organizers for accepting a School Team in their challenge
407 and to have provided their dataset. We are also grateful for the help from our scientist partners:
408 Anne Deschamps, Fabrice Peix, Jérôme Chèze (Laboratoire Géoazur), and Aymeric Spiga
409 (Laboratoire de Météorologie Dynamique) for their help and support. InSight Education
410 activities are supported by CNES. This is InSight contribution number: ICN 97. We also are
411 grateful to the reviewers, and especially to Jennifer Hecker for reviewing the English language
412 and grammar used.

413

414

415 **References**

- 416 Bigot-Cormier Florence and Jean-Luc Berenguer (2017). How students Can Experience
417 Science and Become Researchers: Tracking MERMAID Floats in the Oceans.
418 Seismological Research Letters, Volume 88, Number 2A, doi:10.1785/0220160121.
- 419 Bozdağ, E., Y. Ruan, N. Metthez, A. Khan, K. Leng, M. van Driel,..., and B.W. Banerdt (2017).
420 Simulations of Seismic Wave Propagation on Mars. Space Science Review, Volume
421 211, Issue 1-4, pp 571-594, doi:10.1007/s11214-017-0350-z
- 422 Clinton, J., D. Giardini, P. Lognonné, B.W. Banerdt, M. Van Driel, M. Drilleau, ... , and A.
423 Spiga (2017). Preparing for InSight: An Invitation to Participate in a Blind Test for
424 Martian Seismicity. Seismological Research Letters, 88.5, pp. 1290-1302,
425 doi:10.1785/0220170094.
- 426 Courboux, F., J.L. Berenguer, A. Tocheport, M.P Bovin, E. calais, Y. Esnault, ... , and J.
427 Virieux (2012). SISMOS à l'Ecole : A Worldwide Network of Realtime Seismometers
428 in Schools. Seismological Research Letters, volume 83, number 5, September/October
429 2012, doi:10.1785/0220110139.
- 430 Kenda, B., P. Lognonné, A. Spiga, T. Kawamura, S. Kedar, W.B. Banerdt, and R. Lorenz
431 (2017). Modeling of ground deformation and shallow surface waves generated by
432 Martian dust, devils and perspectives for near-surface structure inversion. Space
433 Science review, 211, 501-524, doi:10.1007/s11214-017-0378-0
- 434 Krischer, L., T. Megies, R. Barsch, M. Beyreuther, T. Lecocq, C. Caudron, and J. Wassermann
435 (2015). ObsPy: a bridge for seismology into the scientific Python ecosystem.
436 Computational Science & Discovery 8 (2015) 014003, doi:10.1088/1749-
437 4699/8/1/014003

438 Lomax Anthony (2000). The Orfeus Java Workshop: Distributed Computing in Earthquake
439 Seismology. *Seismological Research Letters*, Volume 71, Number 5, doi:
440 10.1785/gssrl.71.5.589

441 Lognonné, P., W.B. Banerdt, D. Giardini, W.T. Pike, U. Christensen, P. Laudet, ... , and
442 J.Wookey (2019). SEIS: Insight's Seismic Experiment for Internal Structure of
443 Mars. *Space Science Reviews*, 215:12, doi.org/10.1007/s11214-018-0574-6

444 Murdoch, N., D. Mimoun, R.F. Garcia, W. Rapin, T. Kawamura, P. Lognonné, ... , and W.B
445 Banerdt (2017A?). Evaluating the Wind-Induced Mechanical Noise on the InSight
446 Seismometers. *Space Science Reviews*, 211(1–4), 429–455, doi.org/10.1007/s11214-
447 016-0311-y

448 Murdoch, N., B. Kenda, T. Kawamura, A. Spiga, P. Lognonné, D. Mimoun, and W.B. Banerdt
449 (2017B?). Estimations of the seismic pressure noise on Mars determined from Large
450 Eddy Simulations and demonstration of pressure decorrelation techniques for the
451 InSight mission. *Space Science Reviews*, 211,457-483, doi:10.1007/s11214-017-0343-
452 y

453 Panning, M. P., E. Beucler, M. Drilleau, A. Mocquet, P. Lognonné, and W.B. Banerdt (2015).
454 Verifying single-station seismic approaches using Earth-based data: Preparation for data
455 return from the InSight mission to Mars. *Icarus*, 248, 230–242.
456 doi.org/10.1016/j.icarus.2014.10.035

457 Roques A., J.L. Berenguer, and E. Bozdağ (2016). A single geophone to locate seismic events
458 on Mars. EGU General Assembly 2016, held 17-22 April, 2016 in Vienna Austria , id.
459 EPSC2016-5313

460 Spiga, A., F. Forget, S.R. Lewis, and D.P. Hinson (2010). Structure and dynamics of the
461 convective boundary layer on mars as inferred from large-eddy simulations and remote-
462 sensing measurements. *Q. J. R. Meteorol. Soc.* 136, 414–428, doi.org/10.1002/qj.563

463 Spiga, A., D. Banfield, N.A. Teanby, F. Forget, A. Lucas, B. Kenda (2018). Atmospheric
464 Science with InSight. *Space Science Reviews*, 214:109, doi.org/10.1007/s11214-018-
465 0543-0

466 Sohn, F., and T. Spohn (1997). The interior structure of Mars: Implications from SNC
467 meteorites. *Journal of Geophysical Research*, Volume 102, Numero E1, pages 1613-
468 1635

469 Van Driel M., S. Ceylan, J.F. Clinton, D. Giardini, H. Alemany, A. Allam, ... , and Y. Zheng
470 (2019). Preparing for InSight: Evaluation of the Blind Test for Martian Seismicity.
471 *Seismological Research Letters*, doi.org/10.1785/0220180379

472 Zollo, A., A. Bobbio, J.L. Berenguer, F. Courboulex, P. Denton, G. Festa, ... , and D. Giardini
473 (2014). The European Experience of Educational Seismology. In: Tong V. (eds)
474 *Geoscience Research and Outreach. Innovations in Science Education and Technology*,
475 vol 21. Springer, Dordrecht.

476

477

478

479

480

481

482 **Mailing list addresses**

483 Julien Balestra: julien.balestra@univ-cotedazur.fr

484 David Ambrois: david.ambrois@geoazur.unice.fr

485 Jean-Luc Berenguer: Jean-Luc.Berenguer@unice.fr

486 Florence Bigot-Cormier: florence.bigot-cormier@lyceeshanghai.com

487 Françoise Courboux: courboux@geoazur.unice.fr

488 Philippe Lognonné: lognonne@ipgp.fr

489 Lucie Rolland: lrolland@geoazur.unice.fr

490 Martin Van Driel: vandriel@erdw.ethz.ch

491

492

493

494

495

496

497

498

499

500

501

Correct quake detections

date	epicentral distance (km)	magnitude
2019-01-12 20:23:50.66	3026.5	3.8
2019-01-29 00:21:07.83	2630.0	2.9
2019-07-15 04:14:57.37	5379.6	4.3
2019-07-20 22:26:35.77	1274.7	3.6
2019-07-30 00:34:15.52	1337.0	3.0
2019-09-03 12:30:52.88	1042.8	3.0
2019-09-22 00:41:02.23	2082.7	5.0
2019-10-06 04:19:50.47	713.7	2.6
2019-10-24 01:53:56.71	724.6	2.5
2019-11-02 01:21:15.37	3051.0	3.0
2019-11-09 05:50:32.50	3703.6	2.9
2019-11-17 00:25:25.91	4006.5	3.3
2019-11-22 11:41:49.10	6486.5	3.6

Correct impact detections

date	epicentral distance (km)	mass (kg)
2019-10-24 22:45:52	997.1	6484.7
2019-10-25 00:58:47	4245.4	637.7

503 Table 1. Correct detections from the School Team (Van Driel et al., 2019).

504

505

506

507

508 **List of Figure Captions**

509 Figure 1. Map of the School Team. (a) Global view. (b) An enlargement of European Schools.
510 (c) An enlargement of Caribbean Schools (French and Haitian). White diamonds: location
511 marker.

512

513 Figure 2. The April 7, 2014, Mw 4.9 Barcelonnette ((a) and (b)) and the April 16, 2016, Mw
514 7.8 Ecuadorian region earthquakes ((c) and (d)) recorded at the BLOR educational station
515 (southeastern France, epicentral distances of 0.6° and 87.6° respectively). (a) Upper
516 seismogram: raw vertical component signal (50Hz sampling rate). Lower seismogram: raw
517 signal decimated to 2 Hz. (b) An enlargement of the starting record of the earthquake from (a).
518 Note that the amplitude scale for the decimated signal is ten times smaller than the scale for the
519 raw signal. (c) Upper seismogram: raw vertical component signal (50Hz sampling rate). Lower
520 seismogram: raw signal decimated to 2 Hz. (d) An enlargement of the starting record of the
521 earthquake from (c). SR: sampling rate.

522

523 Figure 3. Synthetic marsquake on January 12, 2019 (vertical component). (a) Raw seismogram.
524 (b) Raw seismogram filtered with bandpass filtering from 0.001 Hz to 0.01 Hz. (c) Raw
525 seismogram filtered with bandpass filtering from 0.01 Hz to 1.0 Hz. (d) Raw seismogram and
526 corresponding spectrogram. (e) An enlargement of the black dashed rectangle in (d). Black
527 dashed ellipse: supposed frequency signature of Rayleigh waves.

528

529 Figure 4. Elements for the epicenter location from Rayleigh waves. a) Scheme of the three
530 surface paths corresponding to the t_1 , t_2 , and t_3 arrival times in b). Gray star: surface seismic

531 source. Gray inverted triangle: seismic station. b) Raw synthetic seismogram and corresponding
532 spectrogram on September 22, 2019 (vertical component). This picture comes from a screenshot
533 with SG2K80. LR1, LR2 and LR3: pick of the Rayleigh wave passage at the station. t1, t2, t3:
534 corresponding arrival times.

535

536 Figure 5. Back-azimuth estimation for the event on September 22, 2019. (a) An enlargement of
537 the first P waves on each component, without rotation. (b) New amplitudes computed from a
538 rotation of 65° clockwise. a) and b) are screenshots from SG2K80. E: east component. N: north
539 component. Z: vertical component. (c) Relationships between P wave amplitudes from the three
540 components, azimuth and back-azimuth direction. Azimuth: direction of the first ground motion
541 with 180° ambiguity. Back-azimuth: true direction of the first ground motion determined from
542 the P wave polarity on the vertical component.

543

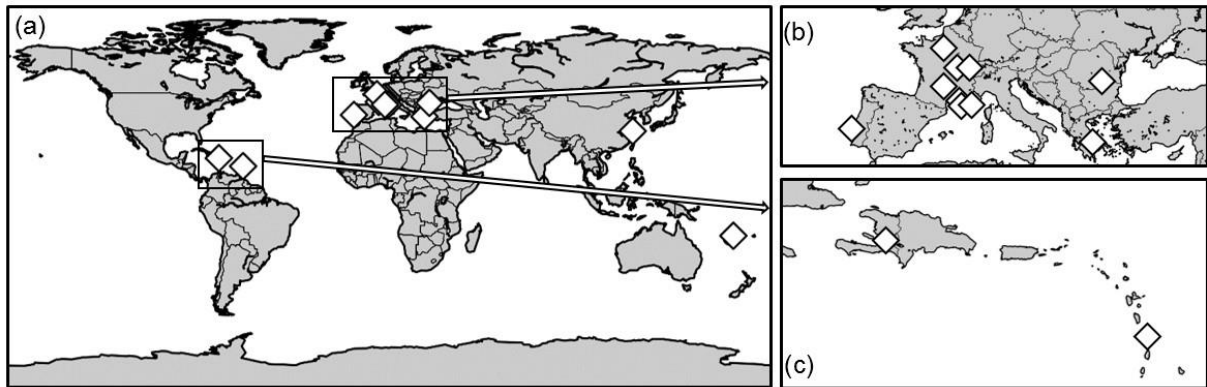
544 Figure 6. Synthetic seismograms from January 10 to January 15, 2019, compiled by a group of
545 students. Vertical black lines: start of a new terrestrial day. Vertical black dashed lines: start of
546 a new martian sol. Double arrows with black dashed vertical segments: marker of the lag
547 between midnight (UTC) and the start of the middle daily event on January 10, 2019. From
548 January 11 to January 15, students observed that the lag increased day after day. E: East
549 component. N: North component. Z: vertical component.

550

551 Figure 7. Study of the unknown event detected by students on July 15, 2019. Raw seismogram
552 filtered with bandpass values from 0.1 Hz to 1.0 Hz and the corresponding spectrogram.
553 Vertical black lines: pick of Rayleigh waves clearly identified in the spectrogram. Vertical black
554 dashed line: pick of LR3 hypothesized by students.

555 **Figures**

556



557

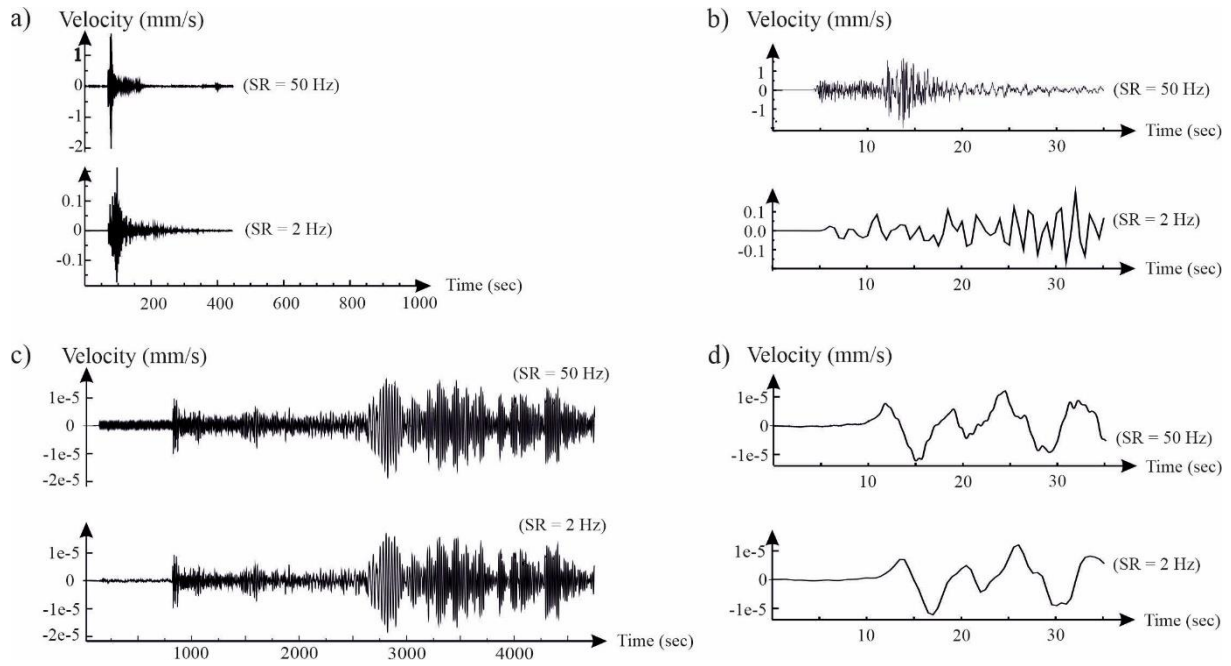
558 Figure 1. Map of the School Team. (a) Global view. (b) An enlargement of European Schools.
559 (c) An enlargement of Caribbean Schools (French and Haitian). White diamonds: location
560 marker.

561

562

563

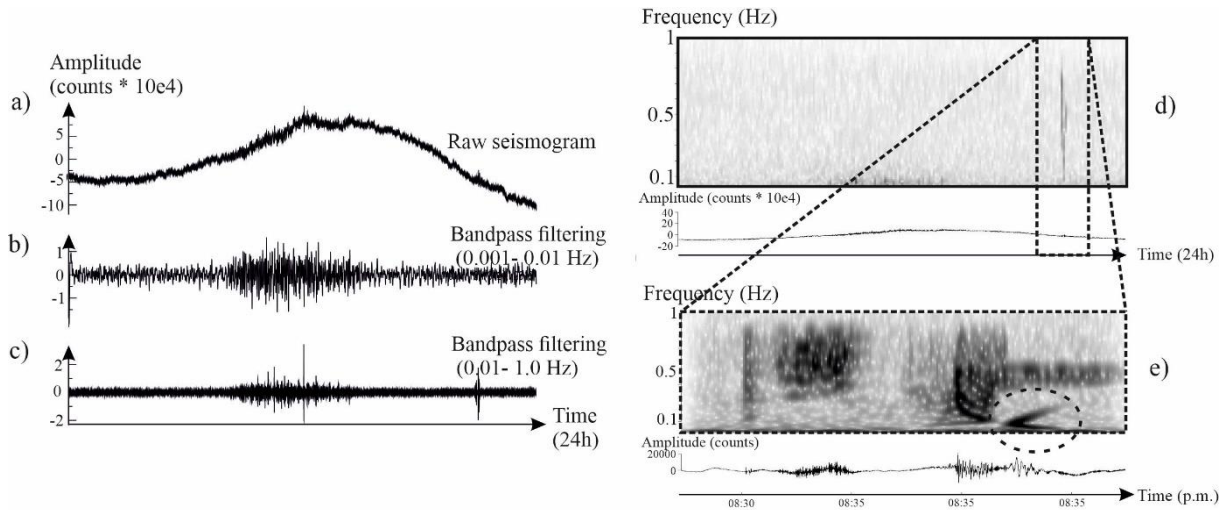
564



565

566 Figure 2. The April 7, 2014, Mw 4.9 Barcelonnette ((a) and (b)) and the April 16, 2016, Mw
 567 7.8 Ecuadorian region earthquakes ((c) and (d)) recorded at the BLOR educational station
 568 (southeastern France, epicentral distances of 0.6° and 87.6° respectively). (a) Upper
 569 seismogram: raw vertical component signal (50Hz sampling rate). Lower seismogram: raw
 570 signal decimated to 2 Hz. (b) An enlargement of the starting record of the earthquake from (a).
 571 Note that the amplitude scale for the decimated signal is ten times smaller than the scale for the
 572 raw signal. (c) Upper seismogram: raw vertical component signal (50Hz sampling rate). Lower
 573 seismogram: raw signal decimated to 2 Hz. (d) An enlargement of the starting record of the
 574 earthquake from (c). SR: sampling rate.

575



576

577 Figure 3. Synthetic marsquake on January 12, 2019 (vertical component). (a) Raw seismogram.
 578 (b) Raw seismogram filtered with bandpass filtering from 0.001 Hz to 0.01 Hz. (c) Raw
 579 seismogram filtered with bandpass filtering from 0.01 Hz to 1.0 Hz. (d) Raw seismogram and
 580 corresponding spectrogram. (e) An enlargement of the black dashed rectangle in (d). Black
 581 dashed ellipse: supposed frequency signature of Rayleigh waves.

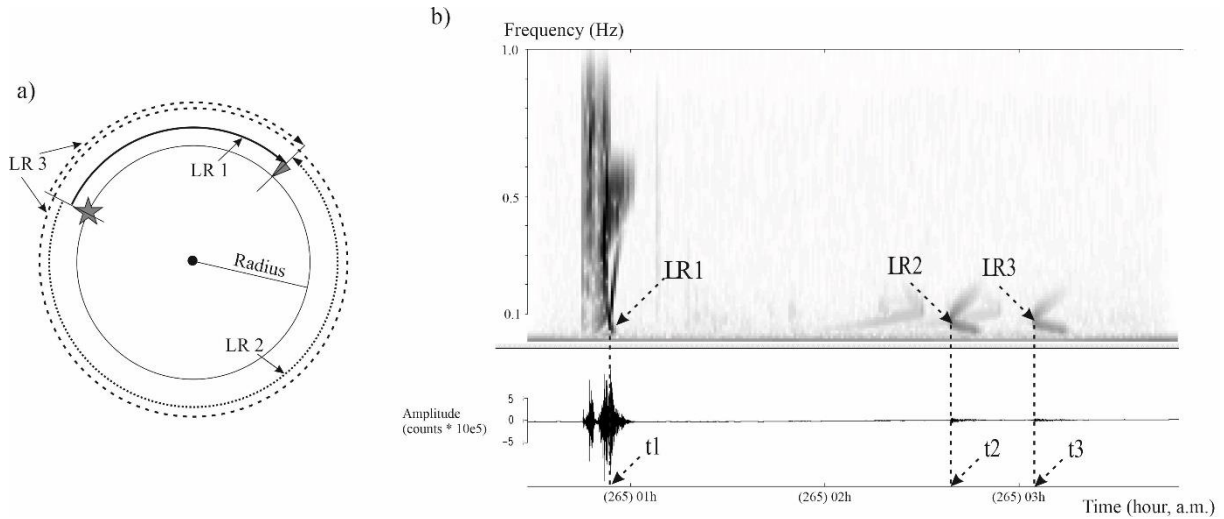
582

583

584

585

586



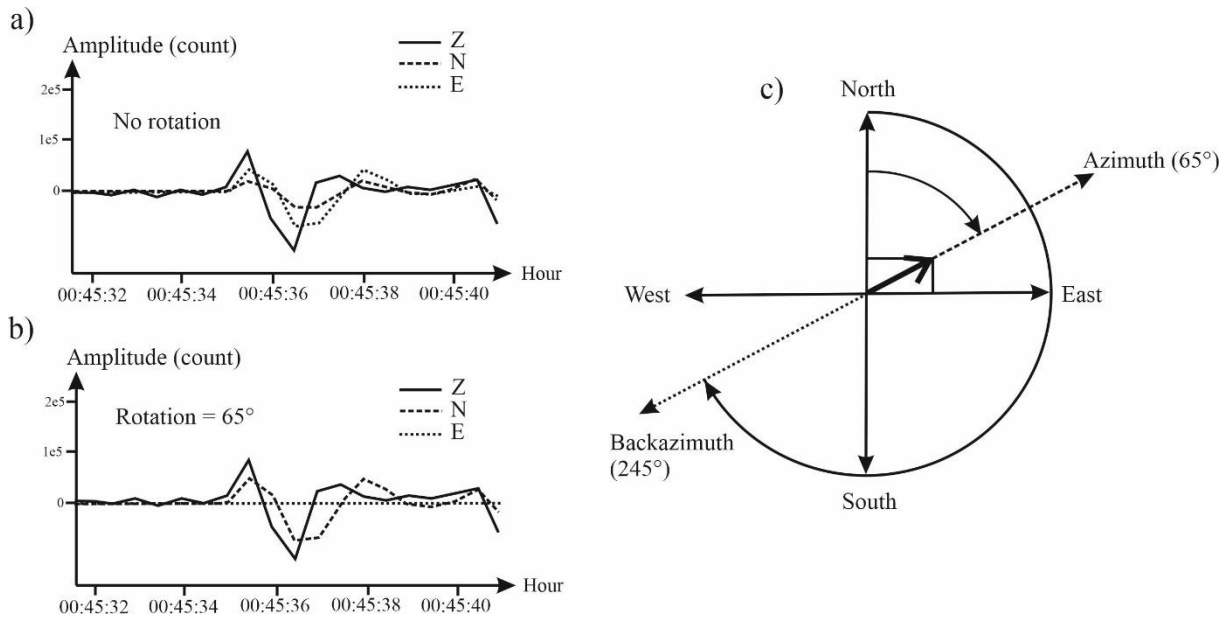
587

588 Figure 4. Elements for the epicenter location from Rayleigh waves. a) Scheme of the
 589 surface paths corresponding to the t1, t2, and t3 arrival times in b). Gray star: surface seismic
 590 source. Gray inverted triangle: seismic station. b) Raw synthetic seismogram and corresponding
 591 spectrogram on September 22, 2019 (vertical component). This picture comes from a screenshot
 592 with SG2K80. LR1, LR2 and LR3: pick of Rayleigh wave passage at the station. t1, t2, t3:
 593 corresponding arrival times.

594

595

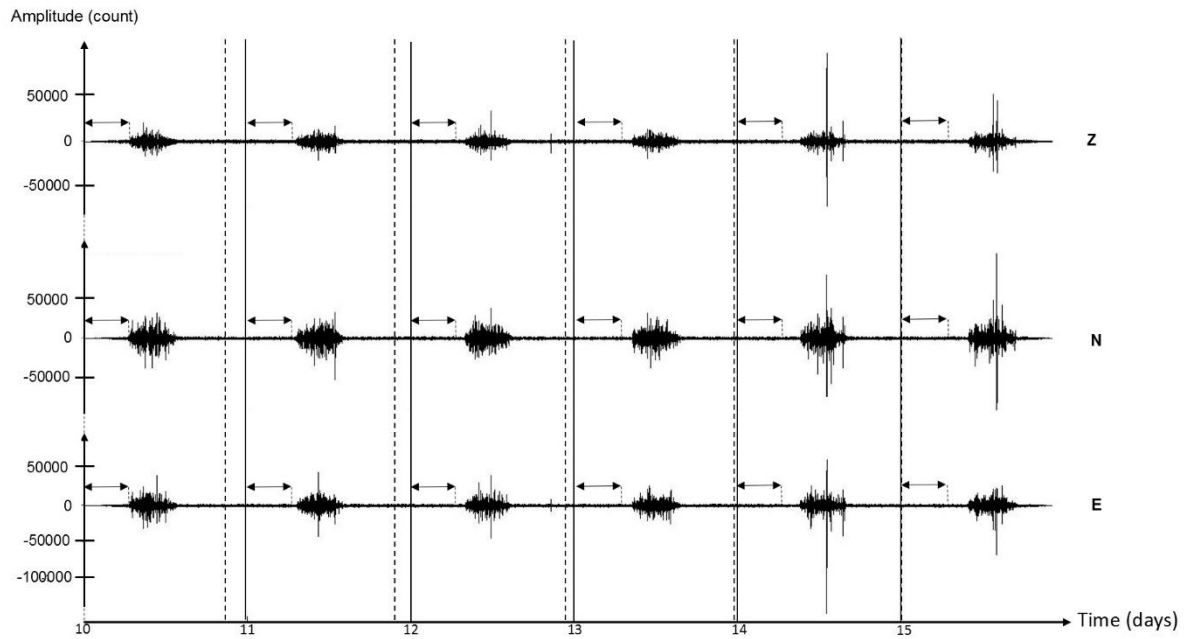
596



597

598 Figure 5. Back-azimuth estimation for the event on September 22, 2019. (a) An enlargement of
 599 the first P waves on each component, without rotation. (b) New amplitudes computed from a
 600 rotation of 65° clockwise. a) and b) are screenshots from SG2K80. E: east component. N: north
 601 component. Z: vertical component. (c) Relationships between P wave amplitudes from the three
 602 components, azimuth and back-azimuth direction. Azimuth: direction of the first ground motion
 603 with 180° ambiguity. Back-azimuth: true direction of the first ground motion determined from
 604 the P wave polarity on the vertical component.

605

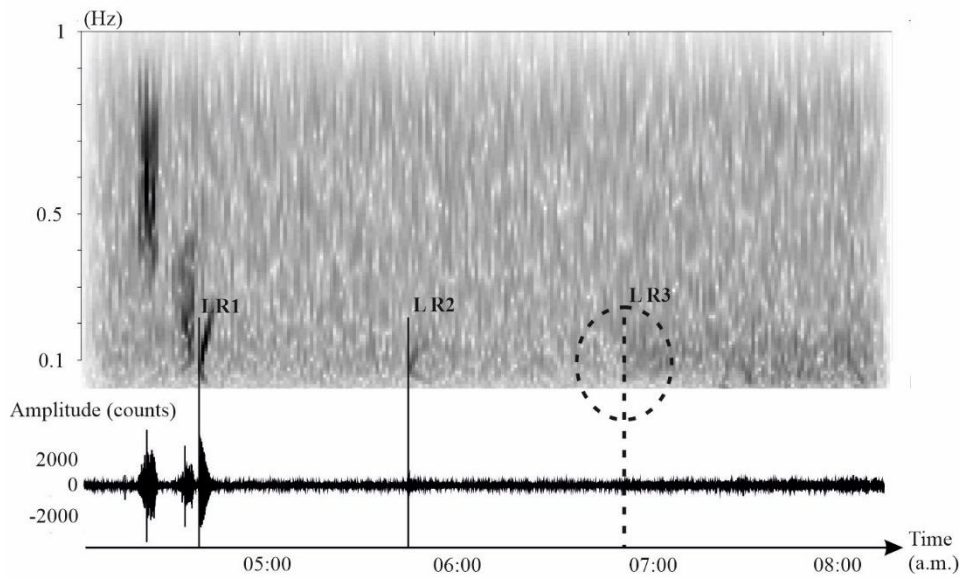


606

607 Figure 6. Synthetic seismograms from January 10 to January 15, 2019, compiled by a group of
 608 students. Vertical black lines: start of a new terrestrial day. Vertical black dashed lines: start of
 609 a new martian sol. Double arrows with black dashed vertical segments: marker of the lag
 610 between midnight (UTC) and the start of the middle daily event on January 10, 2019. From
 611 January 11 to January 15, students observed that the lag increased day after day. E: East
 612 component. N: North component. Z: vertical component.

613

614



615

616 Figure 7. Study of the unknown event detected by students on July 15, 2019. Raw seismogram
 617 filtered with bandpass values from 0.1 Hz to 1.0 Hz and the corresponding spectrogram.

618 Vertical black lines: pick of Rayleigh waves clearly identified in the spectrogram. Vertical black

619 dashed line: pick of LR3 hypothesized by students.